Jurnal Tribologi 35 (2022) 169-185

MYTRIBOS Malaysian Tribology Society

Jurnal Tribologi

Website : jurnaltribologi.mytribos.org e-issn: 2289-7232

Surface quality and absorption properties of polymeric composite (PLA-PCU) fabricated using 3D printing for articular cartilage application

Muhammad Nur Akmal Kazim [1], Mohd Fadzli Bin Abdollah [1,2*], Hilmi Amiruddin [1,2], S. Liza [3], Faiz Redza Ramli [1,2]

[1] Fakulti Kejuruteraan Mekanikal, Universiti Teknikal Malaysia Melaka, Hang Tuah Jaya, 76100 Durian Tunggal, Melaka, MALAYSIA.
[2] Centre for Advanced Research on Energy, Universiti Teknikal Malaysia Melaka, Hang Tuah Jaya, 76100 Durian Tunggal, Melaka, MALAYSIA.
[3] Malaysia-Japan International Institute of Technology, Universiti Teknologi Malaysia, Jalan Sultan Yahya Petra, 54100 Kuala Lumpur, MALAYSIA.
*Corresponding e-mail: mohdfadzli@utem.edu.my

KEYWORD

Polylactic acid
Polycarbonate urethane
3D print
Surface quality
Absorption properties

ABSTRACT

The objective of this study is to investigate the impact of four 3D printing process parameters (i.e., layer thickness, PCU composition, nozzle speed and extruding temperature) on the surface roughness and absorption rate of the mixture of PolyLactic Acid (PLA) and PolyCarbonate Urethane (PCU). The specimen was printed using a Fused Filament Fabrication (FFF) technology. The response surface methodology was used for analysing all the experimental data and developing an effective empirical prediction model. The results of the study indicated that the generated model was not much significant with regards to absorption rate, while it was very significant for the surface roughness response parameter. A detailed analysis of the results indicated that layer thickness was the most significant factor that affected the surface roughness, while PCU composition affected the absorption rate. The optimal surface roughness (2.5400 μm) and absorption rate (0.0470%) of the printing process parameters was obtained when PCU concentration is 10 wt.%, layer thickness 0.1 mm, nozzle speed 15 mm/s and extruding temperature 195℃.

Received 4 March 2022; received in revised form 27 May 2022; accepted 9 July 2022.
To cite this article: Kazim et al. (2022). Surface quality and absorption properties of polymeric composite (PLA-PCU) fabricated using 3d printing for articular cartilage application. Jurnal Tribologi 35, pp.167-185

1.0 INTRODUCTION

Meniscal problems in people are mainly caused due to the degradation of the articular cartilage, which further leads to arthritis and knee pain. This problem affects a majority of elderly people in Malaysia and around the world. It has been noted that knee problems increase with increasing age. There has been a significant increase in knee problems amongst women above 50 years (Cui et al., 2020). The common repair methods used for curing knee issues include suture repair, wherein the torn section in the knee is sewed; and meniscectomy, where the damaged section is removed from the knee (Blom et al., 2018). In addition, some other techniques like meniscal transplants and artificial cartilage implants are also used for resolving knee issues. In the case of a meniscal transplant, the patient receives a transplant from the donor, known as an allograft (Keeffe, 2019); while if the patient receives an artificial cartilage implant, the doctors use articular cartilage or artificial meniscus for replacing the damaged section in the knee (Alaia & Fischer, 2021). Allografts or Autografts can be used for treating articular cartilage damage. If the injury is small, the doctors use the patient's cartilage dowel or bone for repairing the injury. However, if the patient is suffering from a large injury, the doctors need to acquire the cartilage dowel and bone from other donors. Some techniques like drilling, arthroscopy, fixation and bone and cartilage reconstruction are carried out for resolving the damage (Accadbled et al., 2018). Artificial implants are usually fabricated using popular materials like PolyLactic Acid (PLA) and PolyCarbonate Urethane (PCU) (Bagaria et al., 2018; Beckmann et al., 2018; Okolie et al., 2020).

PLA is commonly used in the medical field because of its remarkable physical, chemical and mechanical properties and it is also approved by Food and Drugs Administration (FDA) (Tyler et al., 2016). This material is generally used as a drug carrier, in tissue engineering, orthopaedic, dental and 3D printing (DeStefano et al., 2020). PLA fabrication is used for developing artificial implants with the help of additive or formative manufacturing (Narayanan et al., 2016; Whulanza et al., 2022). However, it has been noted that the existing artificial cartilage implant fabricated using the formative manufacturing process is unable to tolerate the joint lubrication by the weeping mechanism owing to a lack of porosity (Elsner et al., 2010). The weeping mechanism takes place if the artificial cartilages (i.e., meniscus and articular cartilage) face a dynamic load (Araujo Borges et al., 2018). The natural cartilage tissue in the human body is usually porous, thus allowing the absorption and discharge of the synovial fluid, which is the main lubricating material that helps in the loading and unloading of the meniscus. However, the current artificial cartilage is only lubricated using the adsorption process (Majd et al., 2015). Hence, the additive manufacturing technique used for developing artificial medical implants is a promising technique as it develops a porous material that displays a precise implant shape at a lower cost to the patient that can be produced using the in-house equipment, thereby making it very feasible and easily accessible (Martelli et al., 2016). However, the stiffness of PLA (1.0 GPa) is seen to be higher compared to the stiffness of the original articular cartilage (13.6 MPa) (Farah et al., 2016; Gabarre et al., 2014). PCU is another promising material that displays almost similar stiffness (12 MPa) as the articular cartilage, which helps it replicate the contact regions and pressure, similar to the healthy cartilage tissue in the body (Gabarre et al., 2014). Even though it is still not approved by FDA to be used as implant, many studies show promising possibilities of using PCU as artificial implant and other medical used (Wendels & Avérous, 2021). Owing to its stiffness value that mimics certain body part, PCU has garnered a lot of popularity in the medical field, as it also displays significant biostability, biocompatibility and excellent mechanical properties (Inyang & Vaughan, 2020; Vrancken et al., 2013). PCU has been used for developing prosthetic parts, such as artificial knee cartilage. Though the additive manufacturing technique is used for developing

PCU-based components, the manufacturing procedure requires the use of a high-end 3D printer having special nozzles or techniques (Miller et al., 2017). Also, a low stiffness value of PCU increases its ability to wear over time, as a material with a lower stiffness has a low wear resistance (Sivakumar et al., 2021). Earlier studies have indicated that the wear resistance of a material increases if its stiffness value is increased (Friedrich, 2018). Though PCU is a promising material that can be used for developing artificial cartilage implants, additional research needs to be conducted for determining its tribological and material properties (AbdelGaied et al., 2015; Inyang & Vaughan, 2020).

Due to above advantages and disadvantages of both polymers, if the PLA and PCU materials are used for developing a new polymeric mixture, the stiffness of the composite will be higher than that of PCU which will make it more printable with lower cost that PCU and at the same time, the stiffness of the composite will also be lower than that of PLA. This hypothesis is based on (Pachamuthu & Hatna, 2005) which stated that the hardness of polymeric composite will be reduced when a polymer with lower hardness is added to a polymer with a higher hardness. The Fused Filament Fabrication (FFF) process is regarded as an effective 3D printing technique that can be used for many applications, like developing a prototype or model (Norani et al., 2021; Zhang et al., 2020). FFF refers to a printing process where the printing is carried out using the Computer Assisted Drawing (CAD) file, and the filament is deposited layer-wise for generating a model (Rahmati & Vahabli, 2015). The lifespan of the product can be increased if the mechanical and tribological properties of the 3D printed composite PLA-PCU mixture, such as mechanism and characteristics of the contacting surfaces, environment, etc, are further studied and improved.

Hence, this phase of study aims to investigate the influence of different 3D printing process parameters on the absorption properties and surface quality of the polymeric composite mixture (PLA-PCU) as the absorption properties is crucial to sustain the weeping lubrication as in natural cartilage, while the surface quality is critical for good tribological properties (Araujo Borges et al., 2018; Kolawole et al., 2021)This composite material can be used for developing a knee material replacement. The results of this study could present a new knowledge regarding the optimum additive manufacturing parameters of artificial articular cartilage using new polymeric composite that can be used in the medical field for resolving the issues related to increasing human age.

2.0 MATERIALS AND METHODS

2.1 Specimen Preparation

The PCU material was obtained from AdvanSource Biomaterial Corps (USA). This pellet was initially dried in a vacuum oven at 100 ℃ for 10-13 h for removing any moisture. The materials were mixed and extruded using twin screw extruder in Fibre and Biocomposite Development Centre (FIDEC) of Malaysia Timber Industry Board (MTIB). Twin screw extruder is used due to its credibility to completely mix different types of thermoplastic into a 3D filament (Martins & De Paoli, 2005). Then, a sample was designed having a diameter of 12.7 mm and 25.4 mm long, with the help of the SOLIDWORKS software. The design file was saved as a .stl file. The slicing software (FlashPrint) was used for manipulating all printing parameters like layer thickness, PCU composition, nozzle speed and extruding temperature. The different samples were printed using the FlashForge CreaterPro software. Figure 1 presents an example of the 3D printed model after all parameters were set using the Flashprint software. The specification of 3D printer, FlashForge CreaterPro was retrieved from the supplier as in Table 1.

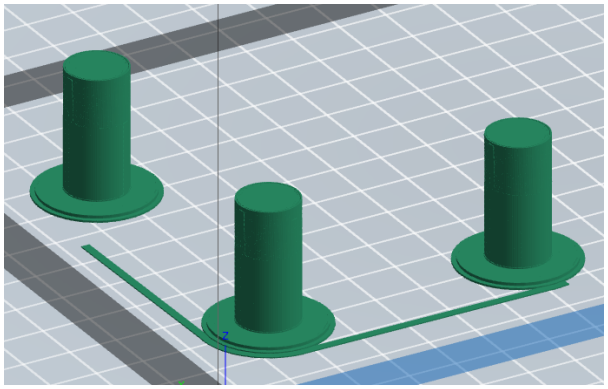

Figure 1: An example of a 3D printed model.

Table 1: The specification of 3D printer.

Nozzle Diameter	0.4mm
Maximum Extruding Temperature	240°C
Print Speed	>100mm/s
Filament Diameter	1.75mm
Layer Thickness	0.1mm-0.4mm
Print Precision	±0.2mm

2.2 Response Surface Methodology

Response Surface Methodology (RSM) refers to a technique that highlights the relationship between different factors and resulting responses based on the data set that is developed for the designed experiments. This technique uses a mathematical model for deriving an optimal response (Izamshah et al., 2018). The Central Composite Design (CCD) of the RSM technique was applied, using the DesignExpert software (ver. 12). The factors that were included in the design were nozzle speed, layer thickness, PCU composition and extruding temperature. These 4 factors were noted could or could not significantly affect the surface roughness quality and absorption rate of the designed samples. The CCD design generated 28 experimental runs that had to be implemented for developing an empirical model that highlighted the effect of the above 4 factors on the response parameters (i.e., surface roughness and rate of absorption). This data was based on 3 values of the data curve, i.e., the lowest value, the centre point value and the maximal value. The centre point data set was repeated 4 times for improving the probability of identifying the most significant factors and assessing the variability of the factors. Table 2 presents the values of the factors that were determined based on the experimental sets.

The composition of PCU was capped at 30% due to the limit of extruding process in FIDEC, where the extrusion was not possible when the composition of PCU was more than 30%. The layer height and the printing speed in (Araujo Borges et al., 2018) were at 0.125mm and 20mm/s respectively. Therefore, to find the optimum values for both perimeters, the values were set lower and higher than the said values for minimum and maximum levels, while the values from that study was set as the median value. However, as FlashForge CreatorPro can only be as precise as 0.01mm, the value for layer thickness was adjusted to compliment the limitation. Since the printing temperature for PLA is between 180°C to 215°C (Coppola et al., 2018) and the extrusion

temperature for PCU is 198.8°C (AdvanSource Biomaterials, 2021), the range was set from 195°C to 215°C to find the most optimum extruding temperature. Other than that, the printing infills and the bed temperature were kept constant at 100% infill and 50°C.

Table 2: Values of the four factors.

Parameter	Symbol	Unit	Variation Levels		
			-1	0	1
PCU Composition	A	wt.%	10	20	30
Layer Thickness	B	mm	0.10	0.13	0.16
Nozzle Speed	C	mm/s	15	20	25
Nozzle Temperature	D	°C	195	205	215

2.3 Surface Roughness Test

The surface roughness was tested with the help of a non-contact 3D Surface Profilometer, Shodensha GR3400. Here, the sample was initially placed on a mechanical stage, followed by adjusting the range for obtaining a clear image of the sample's surface. The researchers used the WinRoof software for measuring and analysing the surface roughness. Readings were obtained at 3 different positions on the sample surface. A total of 5 readings were determined for every sample, and an average surface roughness value was determined. The specification of non-contact 3D Surface Profilometer, Shodensha GR3400 is as in Table 3.

Table 3: Specification of non-contact 3D surface profilometer.

Total Magnification	50×, 100×, 200×, 400×, 600×
Eyepiece Lens	10× (18mm)
Object Lens	Plan apochromat object lens (No cover glass) 5×, 10×, 20×, 40×, 60×
Focus Point's Adjustment	Coaxial Coarse/Fine Focus System (Tension adjustment mechanism, limit stopper, minimum scale 0.002mm)
Lighting	6V 20W halogen lamp (With dimming mechanism)

2.4 Absorption Test

The rate of absorption was determined using the modified ASTM D570 – Water Absorption of Plastic process, where the samples were immersed in Ringer's solution. The Ringers' solution was acquired from Sigma-Aldrich Inc. (USA). Ringer's solution refers to a solution that maintains the osmotic balance for cells, thus imitating the body fluid properties (Hahn et al., 2020). The solution was prepared after dissolving the tablet in a beaker containing deionised water (500 ml), pH was adjusted to 7.0 and the solution was sterilised by autoclaving for 15 mins at 121°C. All preparatory steps were based on the directions and product information provided by the company. Then, the above samples were immersed into the Ringer's solution and their weights were determined every 30 mins for 2 hours, then every hour for the next 4 hours, and at the end of 24 hours. Before weighing the samples, they were dried completely to obtain a constant dry weight.

2.5 Surface Morphology Observations

The samples were cut into their centre for determining the porosity between the different layers. Then, the cross-sections of the cut samples were coated with silver and observed using the Scanning Electron Microscope (SEM).

3.0 RESULTS AND DISCUSSION

Table 4 describes the results of the surface roughness and rate of absorption based on the data included in DesignExpert.

Table 4: Results of the experiments.

	Factors				Responses	
Exp No.	**PCU Comp., A [wt.%]**	**Layer Thickness, B [mm]**	**Nozzle Speed, C [mm/s]**	**Nozzle Temp., D [℃]**	**Roughness, *Ra* [μm]**	**Absorption, *e* [%]**
1	30	0.10	15	215	3.1333	0.0228
2	20	0.13	15	205	4.2933	0.0190
3	30	0.16	15	215	6.3400	0.0360
4	30	0.10	15	195	2.7467	0.0385
5	10	0.16	25	215	7.3533	0.0279
6	20	0.16	20	205	5.5200	0.0321
7	20	0.10	20	205	2.6733	0.0296
8	30	0.13	20	205	4.2800	0.0376
9	20	0.13	20	205	4.6133	0.0326
10	30	0.10	25	195	3.3400	0.0212
11	10	0.13	20	205	5.2600	0.0144
12	20	0.13	20	205	5.8000	0.0656
13	10	0.10	15	215	2.6600	0.1074
14	20	0.13	25	205	4.2733	0.0431
15	20	0.13	20	205	4.1933	0.0554
16	30	0.16	25	195	7.4800	0.0330
17	10	0.10	15	195	2.5400	0.0470
18	30	0.16	15	195	6.7267	0.0410
19	10	0.16	15	195	6.2333	0.0757
20	10	0.16	25	195	6.0800	0.0461
21	20	0.13	20	205	3.9000	0.0326
22	20	0.13	20	215	4.5067	0.0334
23	20	0.13	20	195	4.2133	0.0186
24	10	0.16	15	215	7.5533	0.0241
25	30	0.10	25	215	2.3933	0.0178
26	10	0.10	25	215	2.6200	0.0343
27	10	0.10	25	195	2.4333	0.0440
28	30	0.16	25	215	6.5467	0.0258

3.1 Statistical Analysis

Tables 5 and 6 present the values for the Analysis of Variance (ANOVA) derived for all the experimental sets. Linear process order was chosen to create ANOVA for both responses as both responses exhibit lower p-values when analysed using the said order. This model was regarded as statistically significant at the confidence level of 95% if p-values were <0.05. With regards to the surface roughness, only the layer thickness was seen to be statistically significant (p-value <0.05); whereas the other 3 factors were statistically insignificant. The layer thickness contributed 89.9% to this response factor. The model showed the R^2 of 90.03%, adjusted R^2 of 88.29% and predicted R^2 value of 85.56%. The difference between the Adjusted and Predicted R^2

values was less than 20%, which indicated that these values were in reasonable agreement. Furthermore, the Adeq. Precision value for this model was seen to be >4, which indicated that the model possessed an adequate signal and could be used for navigating the design space. With regards to the rate of absorption, all the factors showed a p-value >0.05, however, the p-value for the PCU composition was seen to be 0.0814, i.e., <0.1. The PCU composition was noted to be a possible important factor that could significantly affect the absorption rate, as it contributed 11.54% to the model. The R^2, adjusted R^2 and predicted R^2 values for the model were seen to be 19.95%, 6.03% and -23.32%, respectively. The predicted R^2 value was negative, which indicated that the overall average value could be a better predictor for this model. Furthermore, the Adeq. Precision value for this model was seen to be >4, which indicated that the model possessed an adequate signal and could be used for navigating the design space.

With regards to the surface roughness, it was seen that the model fitted the experimental data, as it showed an adequate and insignificant lack of fit, with a satisfactory coefficient of determination (R^2) and Adeq. Precision values. However, with regard to the absorption rate, the model did not fit the experimental data. It could not be used for representing the model though it had an adequate and insignificant lack of fit. For ensuring the "Predicted R^2" and "Adjusted R^2" values showed a reasonable agreement, a few insignificant factors were included in the model. These insignificant factors were necessary for preserving the model hierarchy and determining the response surface for various factors.

Table 5: ANOVA values for the surface roughness response factor.

Source	Sum of Squares	df	Mean Square	F-value	p-value	Contribution (%)
Model	69.3100	4	17.3300	51.9100	<0.0001	
Composition, A	0.0036	1	0.0036	0.0107	0.9186	<0.01
Layer thickness, B	69.2000	1	69.2000	207.3300	<0.0001	89.89
Nozzle speed, C	0.0048	1	0.0048	0.0143	0.9058	0.01
Extruding temperature, D	0.0958	1	0.0958	0.2871	0.5972	0.12
Residual	7.6800	23	0.3338			
Lack of Fit	5.5800	20	0.2792	0.4003	0.9110	
Pure Error	2.0900	3	0.6976			
Total	76.9800	27				

R^2=90.03%; Adjusted R^2=88.29%; Predicted R^2=85.56%; Adeq Precision=16.992

Equations 1 and 2 present the empirical model based on the RSM for the surface roughness and rate of absorption response factors. The empirical model is in coded units and is only valid for the designated printing parameters. Even though the Equation 2 is considered invalid due to the higher p-value of the model for rate of absorption, it is still needed as interaction with surface roughness to find the most optimum parameters. The modelled and measured values of surface roughness and rate of absorption are provided in Figure 2. Figure 2(a) represent the experimental and predicted values for surface roughness, while Figure 2(b) represent the experimental and predicted values for the rate of absorption.

$$Ra = -5.45324 + 0.001407\ (A) + 65.35802\ (B) + 0.003259\ (C) + 0.007296\ (D) \quad (1)$$

$$e = 0.12587 - 0.000818\ (A) - 0.038383\ (B) - 0.001316\ (C) - 0.000197\ (D) \quad (2)$$

where *Ra* is surface roughness and *e* is rate of absorption.

Table 6: ANOVA values for the rate of absorption response factor.

Source	Sum of Squares	df	Mean Square	F-value	p-value	Contribution (%)
Model	0.0021	4	0.0005	1.4300	0.2549	
Composition, A	0.0012	1	0.0012	3.3200	0.0814	11.54
Layer thickness, B	<0.0001	1	<0.0001	0.0659	0.7997	<0.01
Nozzle speed, C	0.0008	1	0.0008	2.1500	0.1560	7.69
Extruding temperature, D	0.0001	1	0.0001	0.1936	0.6641	0.96
Residual	0.0083	23	0.0004			
Lack of Fit	0.0075	20	0.0004	1.3500	0.4585	
Pure Error	0.0008	3	0.0003			
Total	0.0104	27				

R^2= 9.95%; Adjusted R^2=6.03%; Predicted R^2=-23.32%; Adeq Precision=4.4464

3.2 Effect of Different Factors on Surface Roughness

Figure 3 presents the perturbation plot graph, which highlights the comparative effect of the factors for the 3D printed sample on the surface roughness. A graph having a steep plot or a higher curvature indicates that the response is very sensitive to the changes in the particular factor. However, a flat graph indicated that the response was not sensitive to the changes occurring in the factors (Kasim et al., 2013). The graphs can be analysed in the DataExpert software for determining the factors that show a maximal effect on the response factor. Figure 4 presents the conversion of the perturbation plot to a 3D surface plot.

It was noted that the layer thickness factor displayed the steepest plot, indicating that the surface roughness was quite sensitive to the changes. However, the graphs for PCU composition, nozzle speed and extruding temperature were flat and showed a similar plot. Based on the data indicated in the graphs, the layer thickness factor was seen to be a very significant factor that affected the surface roughness. There was an increase in the surface roughness when the layer thickness increased from 0.1 to 0.16 mm. This result was similar to that presented earlier (Norani et al., 2021), which showed that the surface quality was increased if the layer thickness was decreased. However, one study (Wang et al., 2019) mentioned that a low layer thickness decreased the surface quality. These results were attributed to the inappropriate nozzle size that was selected, as a higher pressure was required for squeezing the filament, which deteriorated the surface morphology.

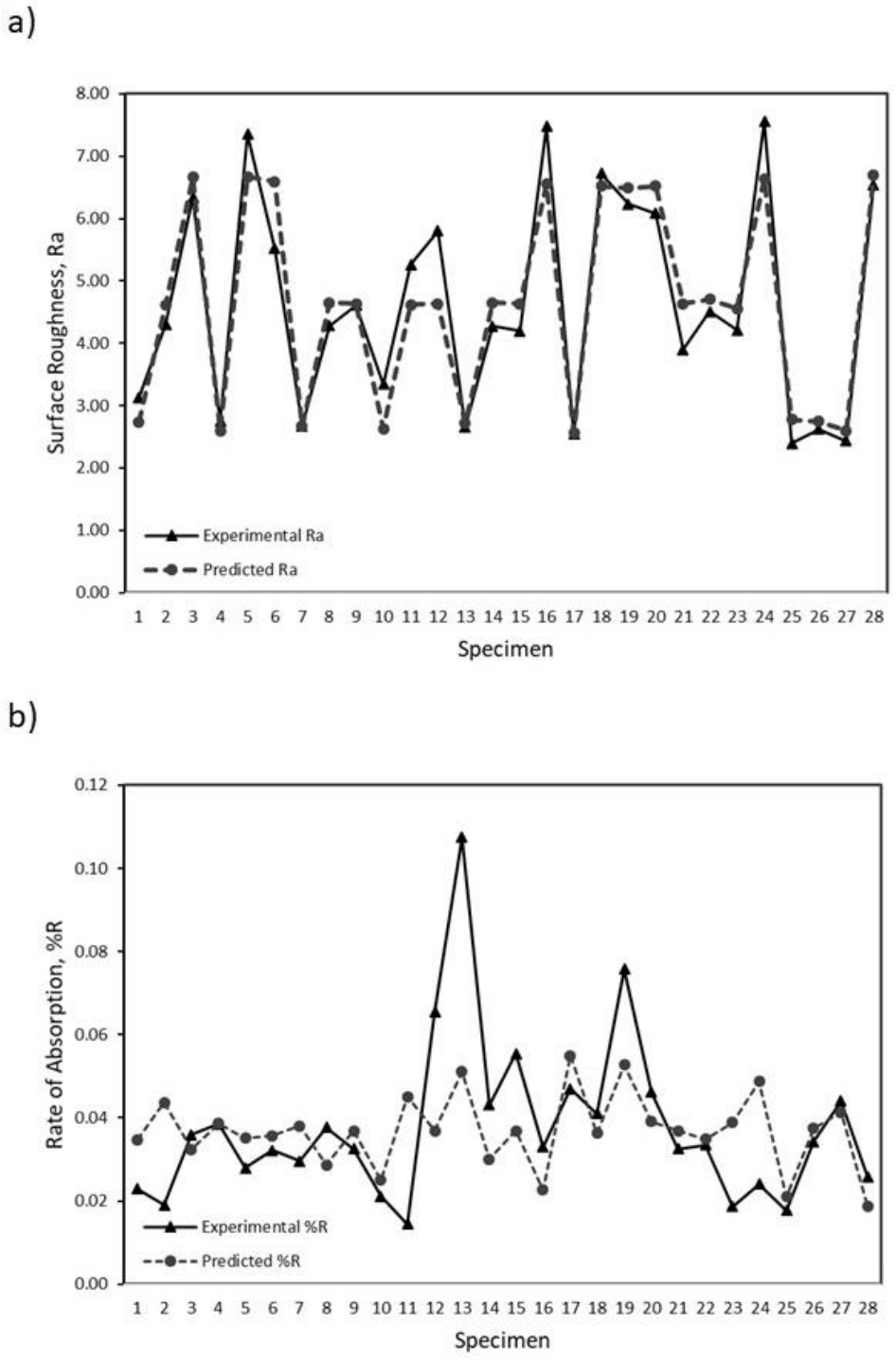

Figure 2: Measured vs. modelled values for (a) surface roughness and (b) rate of absorption.

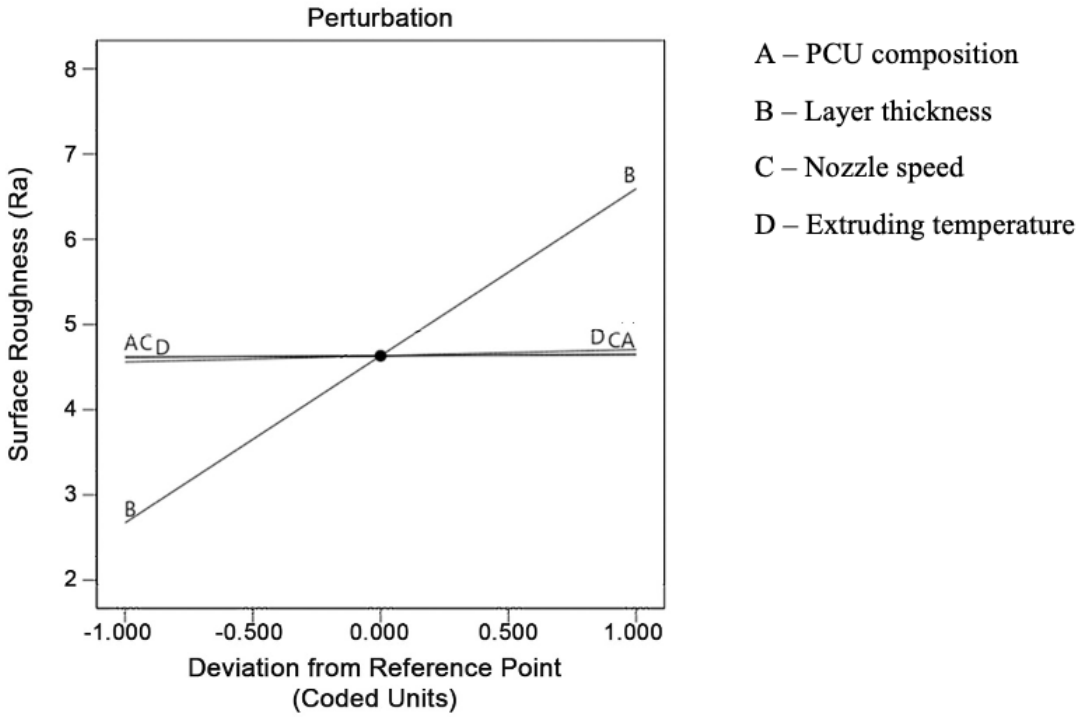

Figure 3: Perturbation graph for surface roughness.

3.3 Effect of Different Factors on the Absorption Rate

Figure 5 presents the perturbation plot that highlights the comparative effects of various factors for the 3D sample on the absorption rate. This plot is different from the plot for surface roughness. The significant factor that affecting the absorption rate could not be determined by just using the perturbation plot, however, it is noted that the plots for the nozzle speed and PCU composition were slightly inclined and very similar. However, the graphs plotted for layer thickness and extruding temperature were almost flat, with no inclination. Therefore, the ANOVA for the rate of absorption was referred to find the most significant factor for the rate of absorption. However, even from the ANOVA, it was noted that the factors were not significant. Nevertheless, the composition of PCU, which has the most percentage of contribution (11.54%) might affect the porosity of the 3D printed sample.

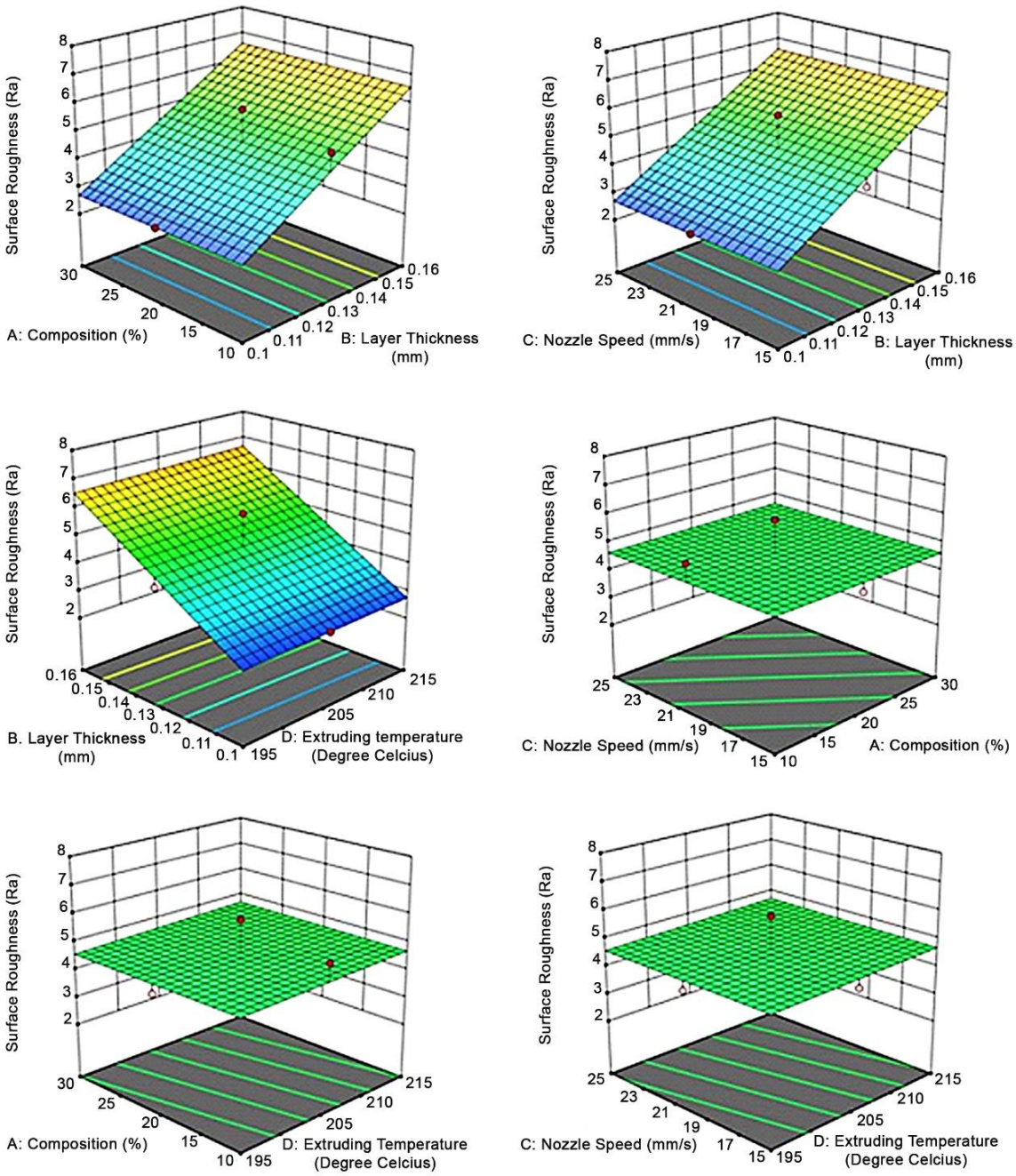

Figure 4: 3D surface plot highlighting the effect of printing process factors on surface roughness.

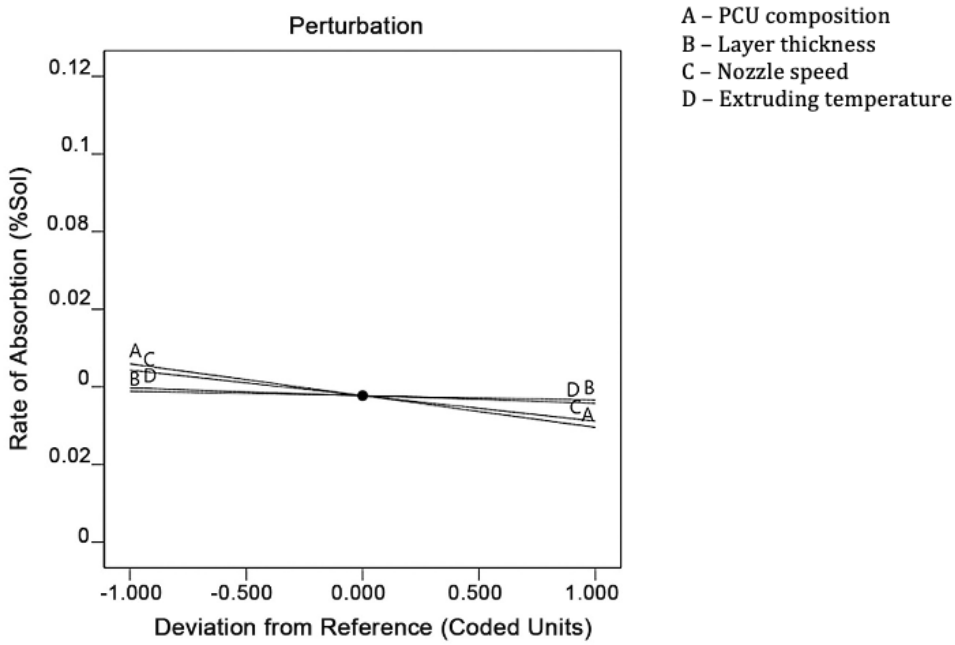

Figure 5: Perturbation graph for the rate of absorption.

Figure 6 presents the translation of the perturbation plots to the 3D surface plots. The curvature of graph in 3D plot were also showed very slight changes between graphs, even when each of the graph was plotted between different factors. Hence, it was a clear indication that the factors had very little effect and were not significant to affect the porosity of the 3D printed samples even though each sample had displayed the ability to absorb the Ringer's solution. This is an agreement with (Delgado et al., 2022) where different types of polymeric composite showed insignificant difference in porosity of printed samples.

3.4 Optimisation of the Response Parameters:

The desirability approach was considered to be the best technique for determining the optimal values of different factors for the desirable response (Chakala et al., 2019). The desirability value ranges between 0 and 1, wherein 0 is the least desirable value while 1 is idle. If the results showed a higher desirability value, it indicated that the response generated more optimal values and could better represent the model (Srivastava et al., 2017).

The multi-response optimisation technique was selected for identifying a sample with minimal surface roughness and maximal absorption rate, simultaneously. Figure 7 and Table 5 present the results of the multi-response optimisation technique. The results indicated the optimal surface roughness and absorption rate values of 2.5400 μm and 0.0470%, respectively, when the layer thickness, nozzle speed and extruding temperature values for the PLA-PCU composite were 10 wt.%, 0.1 mm- 15 mm/s and 195°C, respectively. The results were further validated by conducting confirmatory experiments and all results are presented in Table 5 with acceptable errors below 15%.

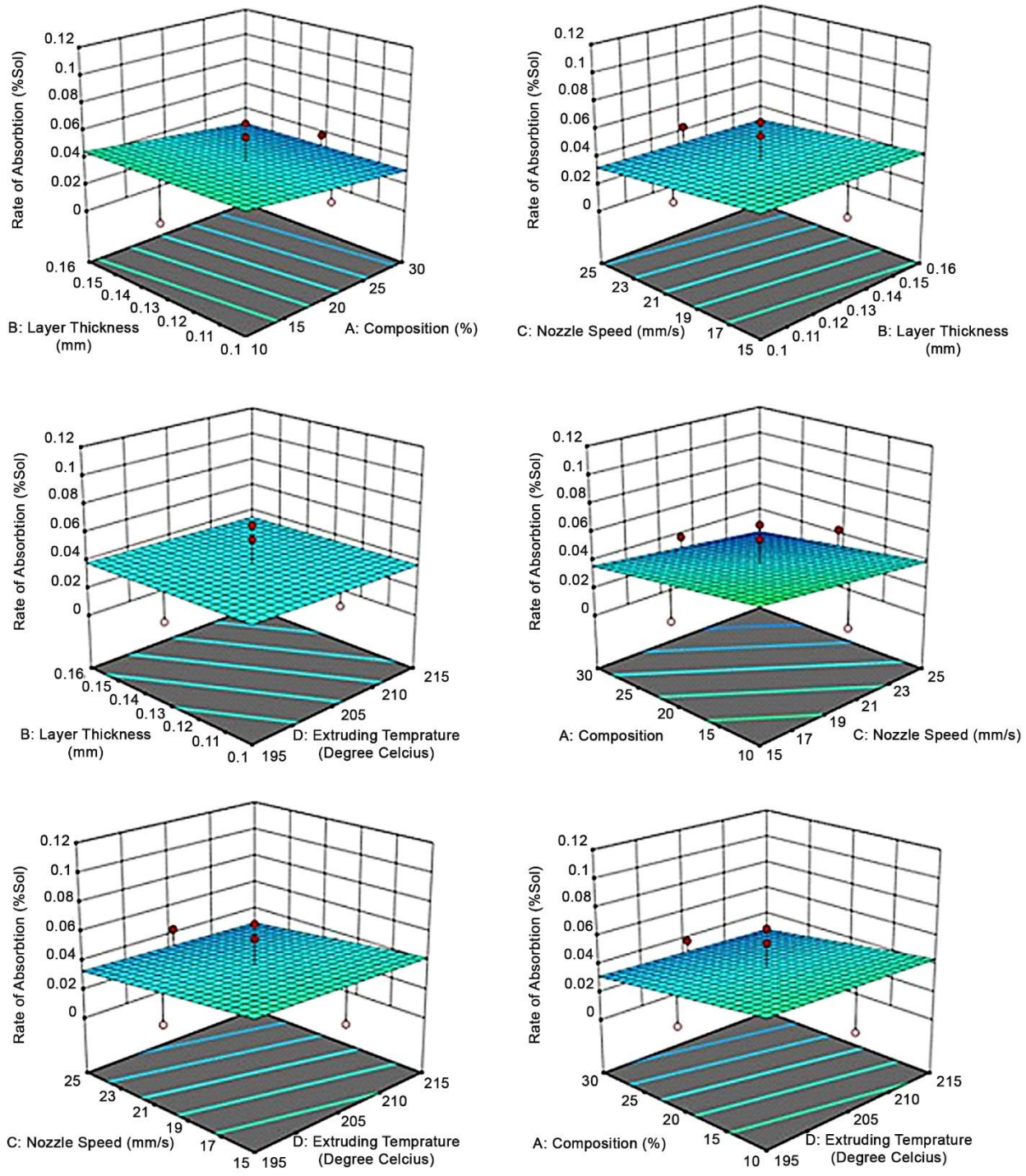

Figure 6: 3D surface plots showing the effect of printing process factors on the absorption rate.

3.5 Surface Morphology Observations

The porosity of the composite sample was determined after controlling the printing infill at 100%. The samples were sliced and analysed using the SEM technique. The arrows in Figure 7 shows the hollow sections or gaps between the layers of filament of the sample, indicating that the sample was porous. This proved that the results of ANOVA for rate of absorption which indicated that the printing process factors did not significantly affect the porosity of the sample due to the present of gaps in the samples. Therefore, if we discard the composition differences, the result was in an agreement with Elsner (2010) where the porosity present even when the printing infill is 100%.

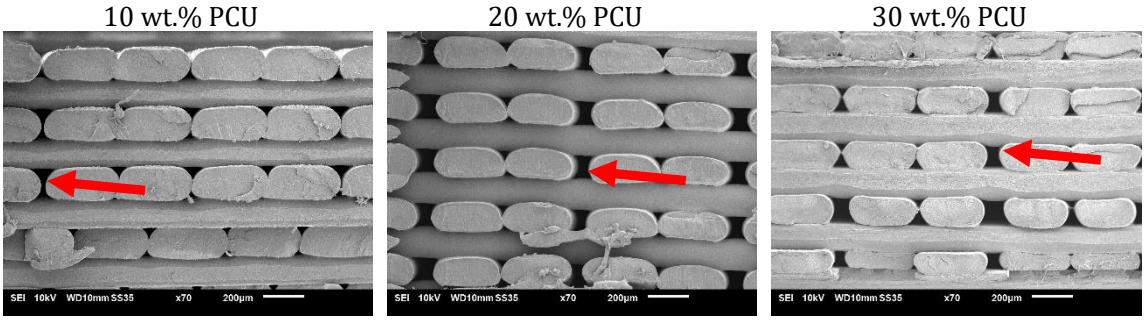

Figure 7: SEM analysis of the samples developed using 3 different PCU compositions.

CONCLUSIONS

In this study, the modelling characteristics of the 3D printed samples were developed with the help of the Central Composite Design (CCD) and the multi-optimum printing parameters was achieved.

(a) The optimised model was seen to be significant for the surface roughness (p-value <0.05) and could be used for assessing the performance of different samples. However, the model was not significant for the rate of absorption (as p-values >0.05). Despite these results, the statistical CCD technique highlighted the interaction between the selected factors and responses.

(b) The layer thickness was seen to be the most significant factor that affected the surface roughness. Thus, the surface roughness could be decreased if layer thickness was lowered. However, the PCU composition significantly affected the rate of absorption. ANOVA stated that a sample with a high PCU composition showed a lower absorption rate.

(c) The layer thickness was seen to be the most significant factor that affected the multi-response optimisation, since it showed a higher ratio of the sum of squares of factor values to the total sum of squares value.

(d) Though PCU composition did not significantly affect both the responses, it still highlighted the interaction and relationship with other factors.

(e) The optimised sample that was determined using the multi-response optimisation parameters (PCU concentration = 10 wt.%, layer thickness = 0.1 mm, nozzle speed = 15 mm/s and extruding temperature = 195°C) showed the optimal surface roughness and rate of absorption values of 2.5400 µm and 0.0470%, respectively with the desirability value of 0.654.

(f) It was noted that the predicted surface roughness value was similar to the experimental value, with a 1.1% reliability. However, the ratio of the predicted and experimental values for the absorption rate response factor was acceptable with a 14.55% reliability value. Nonetheless, the optimum layer thickness (0.1mm) in this study is limited by the specification of the current 3D printer used. Therefore, a further study should be done using lower layer thickness, should there be an FDM 3D printer with a better specification in the future. More mechanical and tribological testing such as compression test, hardness test and etc should be done to further understand the mechanical and tribological behaviour of multi-optimised 3D printed sample that is to be used as artificial articular cartilage implant.

ACKNOWLEDGEMENTS

This study is supported by a grant from Ministry of Higher Education Malaysia (Grant no.: FRGS/1/2020/TK0/UTEM/03/4). The authors gratefully acknowledge use of the services and facilities of the Universiti Teknikal Malaysia Melaka.

REFERENCES

AbdelGaied, A., Stanley, M., Galfe, M., Berry, H., Ingham, E., & Fisher, J. (2015). Comparison of the Biomechanical Tensile and Compressive Properties of Decellularised and Natural Porcine Meniscus. *Journal of Biomechanics*. https://doi.org/10.1016/j.jbiomech.2015.02.044

Accadbled, F., Vial, J., & Sales de Gauzy, J. (2018). Osteochondritis dissecans of the knee. *Orthopaedics and Traumatology: Surgery and Research*, *104*(1), S97–S105. https://doi.org/10.1016/j.otsr.2017.02.016

AdvanSource Biomaterials. (2021). *ChronoFlex C®*. http://www.advbiomaterials.com/products/polycarbonate/chronoflex_c.html

Alaia, M. J., & Fischer, S. J. (2021). *Meniscal Transplant Surgery*. American Academy of Orthopaedic Surgeons. https://orthoinfo.aaos.org/en/treatment/meniscal-transplant-surgery/

Araujo Borges, R., Choudhury, D., & Zou, M. (2018). 3D printed PCU/UHMWPE polymeric blend for artificial knee meniscus. *Tribology International*, *122*, 1–7. https://doi.org/10.1016/j.triboint.2018.01.065

Bagaria, V., Bhansali, R., & Pawar, P. (2018). 3D printing- creating a blueprint for the future of orthopedics: Current concept review and the road ahead! *Journal of Clinical Orthopaedics and Trauma*, *9*(3), 207–212. https://doi.org/10.1016/j.jcot.2018.07.007

Beckmann, A., Heider, Y., Stoffel, M., & Markert, B. (2018). Assessment of the viscoelastic mechanical properties of polycarbonate urethane for medical devices. *Journal of the Mechanical Behavior of Biomedical Materials*, *82*(March), 1–8. https://doi.org/10.1016/j.jmbbm.2018.02.015

Blom, A., Warwick, D., & Whitehouse, M. R. (Eds.). (2018). *Apley & Solomons's: System of Orthopaedics and Trauma* (Tenth). CRC Press.

Chakala, N., Chandrabose, P. S., & Rao, C. S. P. (2019). Optimisation of WEDM parameters on Nitinol alloy using RSM and desirability approach. *Australian Journal of Mechanical Engineering*, *00*(00), 1–13. https://doi.org/10.1080/14484846.2019.1681239

Coppola, B., Cappetti, N., Maio, L. Di, & Scarfato, P. (2018). *Samples Properties*. 1–17. https://doi.org/10.3390/ma11101947

Cui, A., Li, H., Wang, D., Zhong, J., Chen, Y., & Lu, H. (2020). Global, regional prevalence, incidence and risk factors of knee osteoarthritis in population-based studies. *EClinicalMedicine*, *29–30*, 100587. https://doi.org/10.1016/j.eclinm.2020.100587

Delgado, G. F., Pinho, A. C., & Piedade, A. P. (2022). *3D Printing for Cartilage Replacement A Preliminary Study to Explore New Polymers Enhanced Reader*. MDPI. https://doi.org/https://doi.org/10.3390/polym14051044

DeStefano, V., Khan, S., & Tabada, A. (2020). Applications of PLA in modern medicine. *Engineered Regeneration*, *1*(September), 76–87. https://doi.org/10.1016/j.engreg.2020.08.002

Elsner, J. J., Portnoy, S., Zur, G., Guilak, F., Shterling, A., & Linder-Ganz, E. (2010). Design of a free-floating polycarbonate-urethane meniscal implant using finite element modeling and experimental validation. *Journal of Biomechanical Engineering*, *132*(9), 1–8. https://doi.org/10.1115/1.4001892

Farah, S., Anderson, D. G., & Langer, R. (2016). Physical and mechanical properties of PLA, and their functions in widespread applications — A comprehensive review. *Advanced Drug Delivery Reviews*, *107*, 367–392. https://doi.org/10.1016/j.addr.2016.06.012

Friedrich, K. (2018). Polymer composites for tribological applications. *Advanced Industrial and Engineering Polymer Research*, *1*(1), 3–39. https://doi.org/10.1016/j.aiepr.2018.05.001

Gabarre, S., Herrera, A., Mateo, J., Ibarz, E., Lobo-Escolar, A., & Gracia, L. (2014). Study of the Polycarbonate-Urethane/Metal Contact in Different Positions during Gait Cycle. *BioMed Research International*, *2014*. https://doi.org/10.1155/2014/548968

Hahn, R. G., Drobin, D., Li, Y., & Zdolsek, J. (2020). Kinetics of ringer's solution in extracellular dehydration and hemorrhage. *Shock*, *53*(5), 566–573. https://doi.org/10.1097/SHK.0000000000001422

Inyang, A. O., & Vaughan, C. L. (2020). Functional characteristics and mechanical performance of PCU composites for knee meniscus replacement. *Materials*, *13*(8). https://doi.org/10.3390/MA13081886

Izamshah, R., Akmal, M., Ali, M. A., & Kasim, M. S. (2018). Performance evaluation of rotary mechanism characteristics by response surface methodology in cylindrical wire electrical discharge turning. *Advances in Materials and Processing Technologies*, *4*(2), 281–295. https://doi.org/10.1080/2374068X.2017.1418583

Kasim, M. S., Che Haron, C. H., Ghani, J. A., & Sulaiman, M. A. (2013). Prediction surface roughness in high-speed milling of Inconel 718 under Mql using Rsm method. *Middle East Journal of Scientific Research*, *13*(3), 264–272. https://doi.org/10.5829/idosi.mejsr.2013.13.3.1780

Keeffe, P. (2019). *New Medical Device May Eliminate Need for Some Knee Replacement Surgery*. Healthline Media. https://www.healthline.com/health-news/artificial-meniscus-procedure-knee-surgery-less-painful

Kolawole, F. O., Kolawole, S. K., Varela, L. B., Kraszczuk, A., Ramirez, M. A., & Tschiptschin, A. P. (2021). Effect of substrate surface roughness on the tribological properties of dlc-h coatings on tappet valve. *Tribology in Industry*, *43*(2), 189–199. https://doi.org/10.24874/ti.927.07.20.11

Majd, S. E., Kuijer, R., Schmidt, T. A., & Sharma, P. K. (2015). Role of hydrophobicity on the adsorption of synovial fluid proteins and biolubrication of polycarbonate urethanes: Materials for permanent meniscus implants. *Materials and Design*, *83*, 514–521. https://doi.org/10.1016/j.matdes.2015.06.075

Martelli, N., Serrano, C., Van Den Brink, H., Pineau, J., Prognon, P., Borget, I., & El Batti, S. (2016). Advantages and disadvantages of 3-dimensional printing in surgery: A systematic review.

Surgery (United States), *159*(6), 1485–1500. https://doi.org/10.1016/j.surg.2015.12.017
Martins, C. R., & De Paoli, M. A. (2005). Antistatic thermoplastic blend of polyaniline and polystyrene prepared in a double-screw extruder. *European Polymer Journal*, *41*(12), 2867–2873. https://doi.org/10.1016/j.eurpolymj.2005.06.016
Miller, A. T., Safranski, D. L., Smith, K. E., Sycks, D. G., Guldberg, R. E., & Gall, K. (2017). Fatigue of injection molded and 3D printed polycarbonate urethane in solution. *Polymer*, *108*, 121–134. https://doi.org/10.1016/j.polymer.2016.11.055
Narayanan, G., Vernekar, V. N., Kuyinu, E. L., & Laurencin, C. T. (2016). Poly (lactic acid)-based biomaterials for orthopaedic regenerative engineering. In *Advanced Drug Delivery Reviews* (Vol. 107, pp. 247–276). https://doi.org/10.1016/j.addr.2016.04.015
Norani, M. N. M., Abdullah, M. I. H. C., Abdollah, M. F. Bin, Amiruddin, H., Ramli, F. R., & Tamaldin, N. (2021). Mechanical and tribological properties of fff 3d-printed polymers: A brief review. *Jurnal Tribologi*, *29*(March), 11–30.
Okolie, O., Stachurek, I., Kandasubramanian, B., & Njuguna, J. (2020). 3d printing for hip implant applications: A review. *Polymers*, *12*(11), 1–29. https://doi.org/10.3390/polym12112682
Pachamuthu, P., & Hatna, S. (2005). *Journal of Macromolecular Science , Pure and Applied Chemistry*. *October 2015*. https://doi.org/10.1080/10601320500205764
Rahmati, S., & Vahabli, E. (2015). Evaluation of analytical modeling for improvement of surface roughness of FDM test part using measurement results. *International Journal of Advanced Manufacturing Technology*, *79*(5–8), 823–829. https://doi.org/10.1007/s00170-015-6879-7
Sivakumar, G., Jackson, J., Ceylan, H., & Sundararajan, S. (2021). An investigation on ice adhesion and wear of surfaces with differential stiffness. *Wear*, *476*(January), 203662. https://doi.org/10.1016/j.wear.2021.203662
Srivastava, M., Maheshwari, S., Kundra, T., & Rathee, S. (2017). Multi-Response Optimization of Fused Deposition Modelling Process Parameters of ABS Using Response Surface Methodology (RSM)-Based Desirability Analysis. *Materials Today: Proceedings*, *4*(2), 1972–1977. https://doi.org/10.1016/j.matpr.2017.02.043
Tyler, B., Gullotti, D., Mangraviti, A., Utsuki, T., & Brem, H. (2016). Polylactic acid (PLA) controlled delivery carriers for biomedical applications. *Advanced Drug Delivery Reviews*, *107*, 163–175. https://doi.org/10.1016/j.addr.2016.06.018
Vrancken, A. C. T., Buma, P., & Van Tienen, T. G. (2013). Synthetic meniscus replacement: A review. *International Orthopaedics*, *37*(2), 291–299. https://doi.org/10.1007/s00264-012-1682-7
Wang, P., Zou, B., & Ding, S. (2019). Modeling of surface roughness based on heat transfer considering diffusion among deposition filaments for FDM 3D printing heat-resistant resin. *Applied Thermal Engineering*, *161*(June), 114064. https://doi.org/10.1016/j.applthermaleng.2019.114064
Wendels, S., & Avérous, L. (2021). Biobased polyurethanes for biomedical applications. *Bioactive Materials*, *6*(4), 1083–1106. https://doi.org/10.1016/j.bioactmat.2020.10.002
Whulanza, Y., Azadi, A., Supriadi, S., Rahman, S. F., Chalid, M., Irsyad, M., Nadhif, M. H., & Kreshanti, P. (2022). Tailoring mechanical properties and degradation rate of maxillofacial implant based on sago starch/polylactid acid blend. *Heliyon*, *8*(1), e08600. https://doi.org/10.1016/j.heliyon.2021.e08600
Zhang, P., Wang, Z., Li, J., Li, X., & Cheng, L. (2020). From materials to devices using fused deposition modeling: A state-of-art review. *Nanotechnology Reviews*, *9*(1), 1594–1609. https://doi.org/10.1515/ntrev-2020-0101